Comparative Study of Autoencoder and LSTM-AE for Extreme Temperature Anomaly Detection in Semarang

G K Wijaya[1,*], T C S Nova[1], A Anggraeni[1], M A Yusuf[1] and I Kharisudin[1]

[1] Statistics and Data Science, Universitas Negeri Semarang, Semarang, Indonesia

*Corresponding author's email: galihkjaya15@students.unnes.ac.id

Abstract. Climate change has increased the frequency and intensity of extreme weather events, including heatwaves and cold spells, posing critical risks to public health and urban infrastructure. This study proposes and compares two deep learning frameworks based on Autoencoders, namely the Long Short-Term Memory Autoencoder (LSTM-AE) and the standard Autoencoder (AE), for detecting extreme temperature anomalies using historical daily data from 2005 to 2025 in Semarang City. Unlike conventional anomaly detection methods, the LSTM-AE introduces temporal learning through recurrent memory cells, enabling it to capture sequential temperature dependencies that static AE models cannot. Both models are trained to reconstruct "normal" temperature patterns, with anomalies identified when reconstruction errors exceed the 95th percentile threshold. The results demonstrate that the LSTM-AE more consistently identifies significant heatwave and cold spell events, with seasonal alarm rates that closely align with local climatic transitions. Several detected peaks coincide with historically documented events such as the 2015–2019 El Niño and 2019–2020 transition periods reported by BMKG, confirming climatological relevance. In contrast, the standard AE detects a higher number of anomalies (726 vs 366 from the LSTM-AE) but tends to generate false alarms outside transitional periods. Model performance is evaluated using reconstruction error distributions, Jaccard similarity indices, and monthly alarm rates. This study highlights the potential of LSTM-based architectures for improving anomaly detection in climate data and contributes to developing data-driven strategies for urban climate resilience in tropical regions.
Keyword: anomaly detection, autoencoder, lstm, climate change, extreme temperature.

1. Introduction

In recent years, climate change has increasingly become a major global concern [1]. One of the most evident impacts is the growing intensity and frequency of extreme weather events, such as prolonged heatwaves, severe winters, and unpredictable shifts in rainfall patterns [2], [3]. These conditions pose serious risks not only to ecosystems but also to key sectors, including public health [4], agriculture [5], and the stability of urban infrastructure [6]. According to the 2024 Climate and Air Quality Report for Indonesia released by the Badan Meteorologi Klimatologi dan Geofisika (BMKG), the country recorded its highest annual temperature anomaly to date, with an increase of 0.8°C above the long-term average , based on historical observations from 113 BMKG observation stations from 1981 to 2024 [7].

The city of Semarang, as one of the metropolitan areas on the northern coast of Java, faces a set of unique challenges. Its strategic geographic location, while advantageous, also makes it vulnerable to

urban heat island (UHI) effects, high population density, and intense economic activity—all of which contribute to the increasingly complex impacts of extreme temperature rise. Otherwise, extreme heatwaves and cold spells degrade quality of life, increase climate-related health risks [8], and intensify the burden on energy and healthcare infrastructure [9], [10]. Extreme tempeture events are generally defined as periods when daily maximum or minimum temperatures persistently exceed or fall below the climatological normal by statistically significant margins [11], commonly identified through percentile-based or standard deviation thresholds derived from long-term historical observations [12], [13].

The importance of detecting extreme temperature anomalies is closely linked to the need for early warning systems and climate adaptation policies at both local and global levels [14]. A detection system capable of identifying anomaly patterns at an early stage allows governments and policymakers to implement targeted adaptation measures, including optimizing public health preparedness [15], balancing energy distribution [16], and integrating climate considerations into urban spatial planning [17]. Furthermore, consistently detected temperature anomaly data can serve as a foundation for developing long-term climate adaptation policies, enabling vulnerable cities like Semarang to better prepare for increasingly unpredictable climate dynamics caused by global change.

Isolation Forest (iForest) method has been widely used in temperature anomaly detection due to its simplicity, computational efficiency, and ability to handle large datasets without assuming any specific data distribution. The algorithm operates by constructing random decision trees to isolate outlier data points, where the quicker a point is isolated, the more likely it is to be an anomaly [18]. Its application has proven effective, for instance, in detecting surface temperature anomalies in satellite imagery to identify underground coal fires [19], as well as in detecting temperature sensor anomalies in spacecraft, achieving high detection rates with low false alarms [20]. However, the primary limitation of iForest lies in its inability to capture temporal or seasonal patterns, as each observation is treated independently, without considering intertemporal relationships. This makes it less suitable for climate data, which typically exhibit complex seasonal cycles. Therefore, while iForest is often used as a strong baseline in temperature anomaly detection, deep learning-based approaches such as Autoencoders and LSTM-AE (LSTM-AE) are considered more effective. These methods are capable of learning complex nonlinear representations and long-term dependencies, resulting in more consistent detection that aligns better with the distinct seasonal dynamics of tropical climates.

Deep learning approaches, particularly Autoencoders and LSTM-AE, are becoming increasingly relevant for anomaly detection in daily temperature data due to their ability to capture complex patterns and long-term dependencies in time series. An Autoencoder functions by reconstructing the input and identifying anomalies through reconstruction error, while an LSTM-AE extends this by learning temporal correlations, an essential feature for climate data, which often exhibit both daily and seasonal trends [21]. Comparative studies have shown that LSTM-AE outperform standard Autoencoders, achieving accuracy rates of up to 99% in detecting anomalies in temperature and other sensor data, owing to their ability to retain latent representations over long input sequences [22]. Other research confirms that LSTM-AE remain effective even when applied to real-world sensor data that are noisy, significantly reducing both false positive and false negative rates [23]. This LSTM-AE particularly well-suited for historical data–based daily temperature anomaly detection, especially in tropical climate contexts characterised by distinct seasonal patterns and long-term variability.

Based on this background, the research problem is formulated as follows: how to design a framework for detecting daily extreme temperature anomalies that can accurately identify significant deviations in the historical climate record of Semarang City, and how to compare the performance of a standard Autoencoder (AE) with that of an LSTM-based Autoencoder (LSTM-AE) in capturing anomalies

related to seasonal transitions. The contributions of this study are threefold: (i) establishing a comparative framework between AE and LSTM-AE for extreme temperature anomaly detection, (ii) integrating reconstruction-error thresholding with seasonal evaluation metrics, and (iii) demonstrating the applicability of deep learning methods for supporting climate adaptation in tropical urban contexts.

2. Research Method

To accurately detect extreme temperature anomalies, a model is needed that is not only capable to process historical data, but also understand complex temporal dynamics. Therefore, this research organized through a series of systematic stages start from pre-processing data, development deep learning model, until evaluation model detection performance. This study utilizes daily temperature data Semarang City from 2005-2025 which is obtained through National Centers for Enviromental Information (NCEI), comprising 7,339 daily observation.

Table 1. Representative data used in the study.

Date	TAVG	TMAX	TMIN	PRCP	SNOW	SNWD
2005-01-01	NaN	NaN	NaN	NaN	NaN	NaN
2005-01-02	83.0	NaN	77.0	0.00	NaN	NaN
2005-01-03	82.0	92.0	77.0	NaN	NaN	NaN
2005-01-04	83.0	NaN	NaN	0.43	NaN	NaN
2005-01-05	82.0	NaN	78.0	NaN	NaN	NaN

2.1. Pre processing

The data preprocessing stage was conducted to ensure the quality and consistency of the temperature dataset before modeling. In this study, three key daily temperature variables were utilized: average temperature (TAVG), maximum temperature (TMAX), and minimum temperature (TMIN), as their combination provides a more comprehensive representation of diurnal and extreme temperature dynamics. The dataset, obtained from the National Centers for Environmental Information (NCEI), was originally recorded in Fahrenheit, thus requiring conversion to Celsius for consistency with climatological standards:

$$T(^oC) = (T(^oF) - 32)\,\frac{5}{9} \tag{1}$$

In addition to the unit conversion, some additional steps were also taken. Missing values (NaN) in the daily temperature series were handled using the linear interpolation method, which estimates missing observations based on the temporal trend between adjacent valid data point [24], [25]. This approach preserves the continuity and smoothness of temperature variations over time, minimizing the risk of abrupt artificial jumnps [26]. After interpolation, any remaining missing entries at the beginning or end of the series were removed to ensure complete data integrity. Furthermore, the data is normalized using MinMaxScaler to speed up the convergence process when training the model [27].

Specifically to the LSTM-AE model, the data is organized in the form of a 30 days time window so that the model can learn the temporal depency pattern. Meanwhile, on a standard Autoencoder, input is given in the form of daily data snapshots without taking into account the time sequence context.

2.2. *LSTM-Autoencoder (LSTM-AE)*

The LSTM-Autoencoder architecture is designed to learn the temporal dependance of the time series of average daily temperature [28]. The model accepts inputs of size $X \in R^{n_t x n_f}$ with n_t is length of the time window and n_f number of features. On the encoder part, two layers LSTM used successively with 128 and 64 units. The first layer outputs a sequential representation $h_i^{(1)}$, while the second layer reduces the temporal dimension to a latent vector representation $z \in R^{32}$ through non-linear transformation:

$$h_i^{(1)} = LSTM_{128(X)}, h^{(2)} = LSTM_{64}\left(h_i^{(1)}\right), z = f(h^{(2)}; W), \tag{2}$$

with $f(\cdot)$ is the activation function ReLU and W Dense layer weight.Latent representation z then replicated along the time dimension using the RepeatVector operation, so $Z \in R^{n_i x 32}$. The decoder part projects these sequences back through two LSTM layers with 64 and 128 units, which results in a reconstruction of the $\hat{X}$[29]:

$$\hat{X} = LSTM_{128}(LSTM_{64}(Z)) \tag{3}$$

The final output is mapped with TimeDistributed Dense layer to restore the original dimensions (n_i, n_f).

Model trained with Mean Absolute Error (MAE) function,

$$L = \frac{1}{n_i \cdot n_f} \sum_{i=1}^{n_i} \quad \sum_{j=1}^{n_f} \quad |X_{ij} - \hat{X}_{ij}|, \tag{4}$$

and Adam optimizer with 50 epoch and batch size 128. The number of epochs was set to provide a balance between stability and the risk of overfitting. A batch size value of 128 was also chosen as a compromise between computational efficiency and granularity of weight updates. Hyperparameter tuning techniques such as grid search were not employed in this study, as the primary objective was to compare the structural performance and anomaly detection behavior between the Autoencoder and LSTM-AE models rather than to optimize individual model performance. Nevertheless, the selected parameters were based on preliminary experiments that provided stable and consistent reconstruction results.

2.3. *Autoencoder*

As a baseline, this study uses a Dense layer-based Autoencoder to reconstruct daily temperature patterns without considering temporal dependencies [30]. Input is a vector $x \in R^d$ with $d = n_f$ is the number of vectors daily temperature. The encoder architecture consists of three consecutive Dense layers with 128, 64, and 32 units which uses the activation function ReLU. Latent representation $z \in R^{32}$ obtained through non-linear transformation:

$$h^{(1)} = f(xW_1 + b_1), h^{(2)} = f\left(h^{(1)}W_2 + b_2\right), z = f(h^{(2)}W_3 + b_2) \tag{5}$$

with $f(\cdot)$ is function ReLU. The decorder projects back z through symmetrical layer sized 64 and 128 units, to produce a reconstruction $\hat{x}$ same dimension as the input using sigmoid activation function:

$$\hat{x} = \sigma(zW_d + b_d)$$

(6)

Like LSTM-AE model, This model is trained with the Mean Absolute Error (MAE) (4) with Adam optimizer.

Number of epoch also set as many as 50 and batch size 32. While a validation split of 0.1 allows for consistent monitoring of model performance during training. Activation function usage ReLU in the hidden layer accelerates convergence through sparsity properties [31], while the output layer uses a sigmoid to keep the reconstructed value in the range of [0, 1] after normalization [[32].

2.4. Anomaly Detection & Evaluation

The anomaly detection stage is performed by calculating the reconstruction error between the original input x and reconstruction output $\hat{x}$. The error is computed using Mean Absolute Error (MAE) for each observation (4), with $n_i \cdot n_f$ is the number of features. MAE was selected instead of metrics such as MSE or RMSE because it provides a more robust and interpretable measure of reconstruction deviation, less sensitive to outliers that may arise from short-term fluctuation in temperature data [33], [34]. The error distribution on the training data is used to determine the detection threshold τ, which is set at the 95th percentile. This value was empirically selected as it provided a balanced trade-off between detection sensitivity and false alarm rate compared to the 90th and 99th percentile. Every observation with $L > \tau$ categorized as an extreme temperature anomaly.

Performance evaluation is done through several aspects. First, the reconstruction error distribution is compared to assess the stability of the model [35]. Second, the number of detected anomalies was analyzed to identify potential false alarms, which were validated qualitatively through their alignment with known seasonal transitions rather than labeled ground truth. Third, the alarm rate was examined on a monthly and seasonal basis to evaluate consistency with Semarang's climatic patterns. This multi-year dataset inherently served as a temporal cross-validation framework to ensure robustness against overfitting to specific seasons. In addition, the similarity of anomalies detected by both models was quantified using the Jaccard similarity index, where a higher value indicates consistent detection behavior and a lower value reflects model complementarity that useful for policymakers to gauge detection reliability and uncertainty [36], [37]. Although additional statistical metrics could be incorporated, reconstruction-based evaluation and seasonal consistency are standard practices for unsupervised climate anomaly detection. To formalize this comparison, the Jaccard similarity index is expressed as follows:

$$J(A,B) = \frac{|A \cap B|}{|A \cup B|},$$

(7)

with A and B is the set of detected anomaly dates of each model.

To clarify the interpretation, the evaluation results are visualized through (i) a histogram of the reconstruction error distribution, (ii) a temporal line chart of reconstruction errors with threshold references, and (iii) a monthly alarm rate curve compared with the average monthly temperature. These visualizations collectively highlight both statistical stability and temporal alignment with climatic variations, providing a concise yet sufficient basis for distinguishing meaningful anomaly patterns within the comparative framework of this study.

3. Result and Discussion

Analysis of reconstruction error is fundamental in evaluating both models, namely the LSTM-AE and the standard Autoencoder. The error distribution serves as a diagnostic indicator of the model's ability to reconstruct "normal" data and to distinguish it from anomalies. The underlying hypothesis is that models with higher reconstruction accuracy should yield a more centered and consistent error distribution [38], [39].

3.1. Result

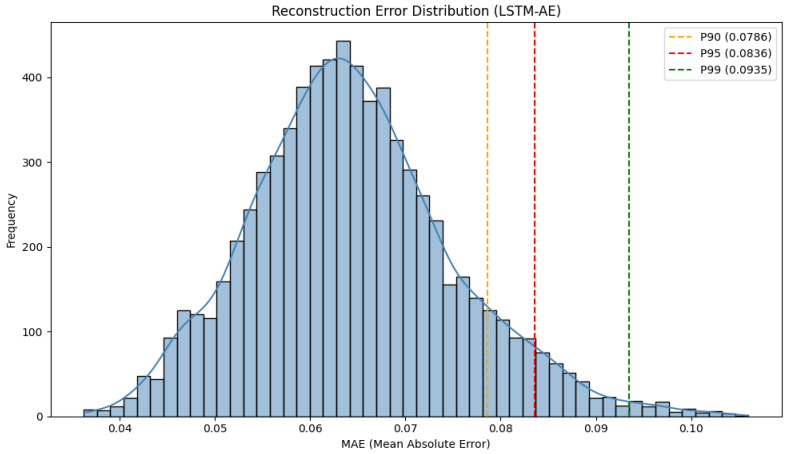

Figure 1. LSTM-AE reconstruction error distribution.

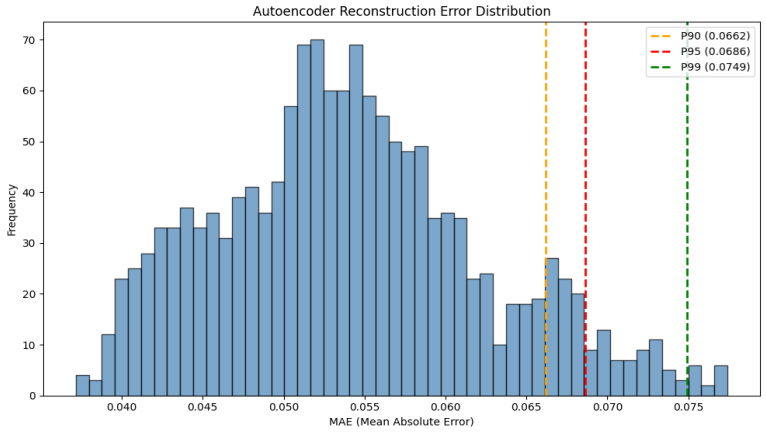

Figure 2. Autoencoder reconstruction error distribution.

The reconstruction error distributions of both models are presented in Figures 1 and 2. Although the standard AE achieves a lower average reconstruction error (approximately 0.04–0.05) compared to the LSTM-AE (around 0.06), this does not directly imply superior anomaly detection capability. The LSTM-AE produces a smoother and unimodal error distribution, while the AE shows a more irregular, bimodal pattern. This indicates that the LSTM-AE reconstructs normal patterns more consistently across temporal variations, reducing random fluctuations that may be misinterpreted as anomalies. Thus, model superiority in this study is determined not by lower absolute error, but by stability and discriminative capacity in distinguishing normal from anomalous behavior [40].

Table 1. Sensitivity of anomaly detection across percentile thresholds.

Percentile (τ)	Threshold Value (MAE)	Detected Anomalies (n)
P-90th	0.0787 (LSTM-AE) / 0.0662 (AE)	726 (LSTM-AE) / 814 (AE)
P-95th	0.0836 (LSTM-AE) / 0.0686 (AE)	366 (LSTM-AE) / 421 (AE)
P-99th	0.0937 (LSTM-AE) / 0.0749 (AE)	71 (LSTM-AE) / 89 (AE)

To assess robustness to the chosen detection thresholds, additional experiments were conducted using the 90th, 95th, and 99th percentiles of the reconstruction error distributions. The 90th percentile produced excessive detections (high false alarm potential), while the 99th percentile was overly restrictive and missed several anomaly clusters. The 95th percentile yielded the most balanced trade-off between sensitivity and stability; therefore, it was selected as the final threshold for both models. Empirically, the 95th percentile corresponded to approximately 5–6% of total daily observations being classified as anomalies, which is consistent with the typical proportion of extreme temperature events reported in global climatological studies (see Table 1). This multi-percentile testing confirms that the reported results are not dependent on an arbitrary choice of threshold, but are consistent across a reasonable range of detection sensitivities.

Since no labeled ground-truth anomaly data were available, false alarms were evaluated contextually rather than through direct label comparison. Specifically, anomalies detected during climatologically stable periods (e.g., months with typical temperature ranges) or inconsistent between models were considered likely false positives. This approach follows established practice in unsupervised climate anomaly studies. [41], [42]. In this context, “noise” is formally defined as short-term fluctuations in daily temperature that remain within the normal climatological range. The standard AE, which processes each day independently, tends to reconstruct such high-frequency variations as separate anomalies, whereas the LSTM-AE captures temporal continuity and suppresses these noisy deviations [43], [44]. Consequently, the LSTM-AE exhibits more robust detection behavior, maintaining consistency across seasons and reducing the number of false alarms under otherwise normal conditions [45].

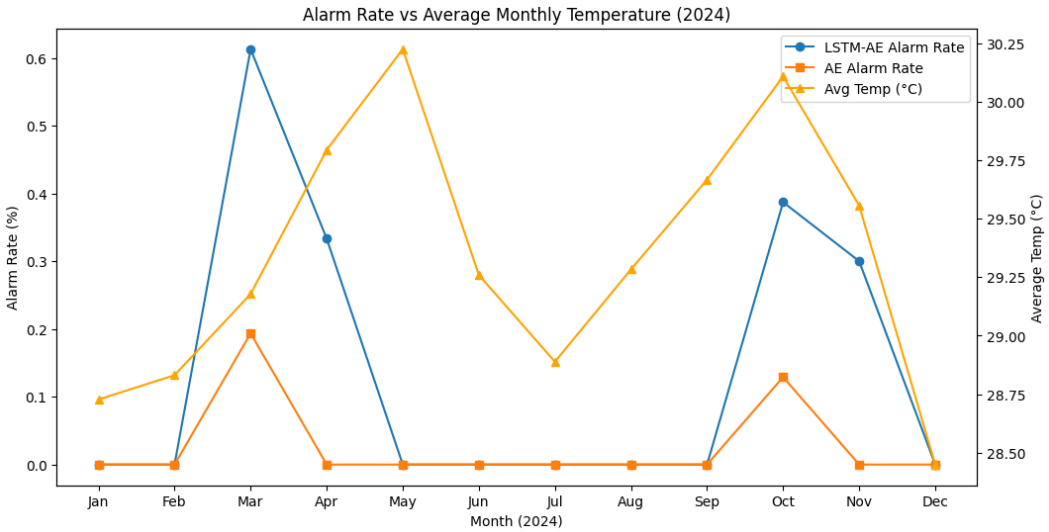

Figure 3. Monthly alarm rate comparison in 2024.

The monthly alarm rate for 2024 reveals distinct detection behaviors between the LSTM-AE and the standard Autoencoder. The LSTM-AE produces higher alarm rates in March (61.3%), April (33.3%), October (38.7%), and November (30%), while other months remain close to zero. Although higher alarm frequencies might suggest over-sensitivity, the temporal alignment of these peaks with known seasonal transitions in Semarang indicates that these alarms correspond to climatologically meaningful events rather than random fluctuations. The detection threshold (τ_{95}) was applied consistently across months to control model sensitivity, confirming that the observed alarm variations arise from genuine temperature dynamics instead of threshold bias.

When compared to the 2024 monthly average temperature (Figure 3), the alarm rate spikes generated by the LSTM-AE align closely with periods of sharp increases or decreases in temperature, particularly in March and October. This correspondence suggests that the model's detections represent seasonal transition anomalies rather than random fluctuations, reinforcing its climatological relevance. In contrast, the standard Autoencoder fails to capture this relationship, its alarm rates are weaker, more sporadic, and largely inconsistent with the dynamics of average temperature. Making it less reliable for supporting climate-based early-warning systems. From an operational perspective, such clustered alarm periods can be interpreted as transition-phase alerts, providing actionable signals for short-term heat-health advisories, adaptive urban cooling measures, and energy demand adjustments in the city's early-warning framework. This translation from model output to practical insight allows policymakers to use detection patterns as early indicators for resource planning and risk mitigation [46], [47].

The Jaccard similarity between both models is 0.156, reflecting limited but meaningful overlap. Rather than indicating spurious detections, this divergence highlights the models' complementary sensitivities: the LSTM-AE captures sequence-dependent anomalies associated with seasonal transitions [48], while the standard Autoencoder responds to short-term reconstruction deviations. This difference arises from their architectural design, as the LSTM-AE incorporates temporal dependencies while the AE treats each day as an independent observation. The consistent seasonal alignment of LSTM-AE alarms confirms that its sensitivity targets meaningful climate events, not random noise. While this study focuses on temperature anomalies, the same architecture could potentially be adapted for other climate variables such as humidity or precipitation, provided that retraining and threshold calibration are performed to account for their distinct temporal behaviors [49]. Consequently, the LSTM-AE demonstrates stronger climatological coherence and practical interpretability, making it a more suitable basis for temperature-oriented early-warning system.

3.2. Discussion

The comparative analysis between the LSTM-AE and the standard Autoencoder highlights key distinctions in their ability to detect extreme temperature anomalies in Semarang City. While the standard Autoencoder exhibits lower average reconstruction errors, it produces a longer-tailed error distribution, which empirically corresponds to a higher frequency of detections during climatologically stable periods—indicating potential false alarms [50]. Although no labeled ground truth anomalies are available, this tendency was validated indirectly by examining the temporal consistency of alarm occurrences: the Autoencoder generated scattered detections even during non-transitional months with minimal temperature variability, unlike the LSTM-AE whose alarms clustered around documented seasonal transition periods [51]. This discrepancy suggests that the long-tail behavior of the AE captures

noise or short-lived fluctuations rather than genuine climatological anomalies, supporting the interpretation of increased false positives arising from its lack of sequential context [52].

In contrast, the LSTM-AE exhibits a more compact rec onstruction error profile with a higher anomaly threshold. This suggests superior robustness in filtering out natural seasonal fluctuations while effectively identifying genuine anomalies, owing to its inherent capacity to model long-term dependencies in time series. As shown in several studies, LSTM-based architectures consistently outperform feedforward Autoencoders in modeling complex environmental or ecological dynamics, particularly those with periodic or fractal characteristics [53], [54]. This temporal awareness enables LSTM-AE to detect abrupt shifts associated with inter-seasonal transitions—such as those observed in March and October in Semarang—while ignoring benign periodic changes.

Nevertheless, the LSTM-AE is not without its challenges. Its deeper architecture leads to higher computational complexity, potential overfitting, and sensitivity to hyperparameters such as time window size, learning rate, and threshold value. Although training is resource-intensive—taking approximately 6 minutes and 44 seconds compared to 16 seconds for the standard Autoencoder—the inference phase remains lightweight, requiring only forward propagation for anomaly scoring. This makes the model practical for periodic or batch-based deployment in early-warning systems. The moderate Jaccard similarity (0.156) also supports a hybrid scheme, where the standard Autoencoder performs baseline monitoring and the LSTM-AE provides high-confidence alerts during transition periods. Such model discrepancies align with previous findings that distinct learning dynamics can yield non-overlapping anomaly sets, which complicates but also enhances ensemble-based validation and deployment [55], [56].

4. Conclusion

This study compared Autoencoder and LSTM-Autoencoder architectures for detecting extreme temperature anomalies in Semarang City using daily data from 2005–2025. The LSTM-AE consistently identified climatologically coherent anomalies aligned with seasonal transitions, while the standard Autoencoder tended to capture short-term fluctuations. Sensitivity testing across the 90th, 95th, and 99th percentile thresholds showed that results remain stable, with the 95th percentile achieving the most balanced trade-off between false alarms and missed detections. Although the Jaccard similarity between models was moderate (0.156), anomalies detected by only one model represent complementary, not inconsistent, signals, each reflecting distinct detection sensitivities. Moreover, several detected peaks coincide with historically documented extreme events—such as the 2015–2019 El Niño and 2019–2020 transition periods—supporting the climatological validity of the proposed method [57].

Despite higher computational demands, the LSTM-AE remains practical for early-warning applications through lightweight inference and periodic deployment. Future research should extend this approach by incorporating additional environmental variables such as humidity, solar radiation, and precipitation to enhance the physical interpretability and temporal robustness of anomaly detection. Integrating multiple features and detection mechanisms may further strengthen the development of adaptive, data-driven climate early-warning systems for tropical urban environments.

References

[1] G. Camps-Valls *et al.*, “Artificial intelligence for modeling and understanding extreme weather and climate events,” *Nature Communications 2025 16:1*, vol. 16, no. 1, pp. 1–14, Feb. 2025, doi: 10.1038/s41467-025-56573-8.

[2] I. Ardian, J. Rawamangun Muka Raya, J. Timur, D. Jakarta, A. Info, and A. History, “ANALISIS SDG 13: DAMPAK PERUBAHAN IKLIM GLOBAL PADA FENOMENA CUACA EKSTREM DI TAHUN 2024,” 2025.

[3] S. NURHALIZAH, "Evaluasi Dampak Perubahan Iklim terhadap Produksi Tanaman Hortikultura," *Circle Archive*, vol. 1, no. 7, May 2025, Accessed: Aug. 18, 2025. [Online]. Available: https://circle-archive.com/index.php/carc/article/view/351

[4] S. Febriosa, W. Sary Pratama, Z. Mahdalena, U. Mahaputra, and M. Yamin, "Analisis Dampak Perubahan Iklim Terhadap Kualitas Lingkungan Hidup Dan Kehidupan Sosial Masyarakat," *MUDABBIR Journal Research and Education Studies*, vol. 5, no. 2, pp. 2211–2221, Jul. 2025, Accessed: Aug. 18, 2025. [Online]. Available: https://www.jurnal.permapendis-sumut.org/index.php/mudabbir/article/view/1480

[5] P. Ramandilla, Z. B, and D. A. Pelly, "DAMPAK PERUBAHAN IKLIM TERHADAP KUALITAS TANAH DAN PRODUKTIVITAS PERTANIAN DI PULAU JAWA," *Jurnal Psikososial dan Pendidikan*, vol. 1, no. 2, pp. 1238–1246, Jul. 2025, Accessed: Aug. 18, 2025. [Online]. Available: https://publisherqu.com/index.php/psikosospen/article/view/2751

[6] R. B. Putra and A. D. Syafei, "ADAPTATION STRATEGIES TO THE IMPACTS OF CLIMATE CHANGE ON ELECTRICITY TRANSMISSION IN THE OPERATIONAL AREA OF PT PLN (PERSERO) UPT PADANG," *Inovasi Pembangunan : Jurnal Kelitbangan*, vol. 13, no. 2, Jul. 2025, doi: 10.35450/JIP.V13I3.1081.

[7] Deputi Bidang Klimatologi, "CATATAN IKLIM DAN KUALITAS UDARA INDONESIA," Jakarta, 2024. Accessed: Aug. 18, 2025. [Online]. Available: https://iklim.bmkg.go.id/id/detail-buletin/?tahun=2025&id=59

[8] J. Wu *et al.*, "The impact of heat waves and cold spells on pneumonia risk: A nationwide study," *Environ Res*, vol. 245, p. 117958, Mar. 2024, doi: 10.1016/J.ENVRES.2023.117958.

[9] S. Zuluaga *et al.*, "Climate change hazards, physical infrastructure systems, and public health pathways," *Environmental Research: Infrastructure and Sustainability*, vol. 3, no. 4, p. 045001, Oct. 2023, doi: 10.1088/2634-4505/ACFABD.

[10] M. R. Khan *et al.*, "Escalating Global Threat of Heatwaves and Policy Options for Adaptation and Mitigation," *Journal of Asian Development Studies*, vol. 13, no. 3, pp. 980–995, Sep. 2024, doi: 10.62345/JADS.2024.13.3.80.

[11] D. Camuffo, A. della Valle, and F. Becherini, "A critical analysis of the definitions of climate and hydrological extreme events," *Quaternary International*, vol. 538, pp. 5–13, Feb. 2020, doi: 10.1016/J.QUAINT.2018.10.008.

[12] C. C. Ibebuchi, C. C. Lee, and S. C. Sheridan, "Recent Trends in Extreme Temperature Events Across the Contiguous United States," *International Journal of Climatology*, vol. 45, no. 2, p. e8693, Feb. 2025, doi: 10.1002/JOC.8693.

[13] L. Brunner and A. Voigt, "Pitfalls in diagnosing temperature extremes," *Nat Commun*, vol. 15, no. 1, pp. 1–9, Dec. 2024, doi: 10.1038/S41467-024-46349-X;SUBJMETA.

[14] C. Lavaysse, C. Cammalleri, A. Dosio, G. Van Der Schrier, A. Toreti, and J. Vogt, "Towards a monitoring system of temperature extremes in Europe," *Natural Hazards and Earth System Sciences*, vol. 18, no. 1, pp. 91–104, Jan. 2018, doi: 10.5194/NHESS-18-91-2018.

[15] H. M. Jones, "Climate Change and Increasing Risk of Extreme Heat," pp. 1–13, 2018, doi: 10.1007/978-3-319-75889-3_1.

[16] H. C. Chen, Q. Han, and B. De Vries, "Modeling the spatial relation between urban morphology, land surface temperature and urban energy demand," *Sustain Cities Soc*, vol. 60, p. 102246, Sep. 2020, doi: 10.1016/J.SCS.2020.102246.

[17] N. Florenzio, G. Guastella, F. Magni, S. Pareglio, and F. Musco, "The role of urban planning in climate adaptation: an empirical analysis of UHI in European cities," *Journal of Environmental Planning and Management*, vol. 66, no. 10, pp. 2071–2089, 2023, doi: 10.1080/09640568.2022.2061334.

[18] D. Cortes, "Revisiting randomized choices in isolation forests," 2021, Accessed: Aug. 23, 2025. [Online]. Available: http://odds.cs.stonybrook.edu/satellite-dataset/

[19] J. Mukherjee, "A Study on Automated Detection of Surface and Sub-Surface Coal Seam Fires Using Isolation Forest from Landsat 8 OLI/TIRS Images," *International Geoscience and Remote Sensing Symposium (IGARSS)*, vol. 2022-July, pp. 5512–5515, Jul. 2022, doi: 10.1109/IGARSS46834.2022.9883726.

[20] M. Bollam, P. H. Roy, A. Jagtap, B. Mullapudi, and A. Verma, "Anomaly Detection in Spacecraft Telemetry using Similarity Metrics and Isolation Forest," *2024 IEEE Space, Aerospace and Defence Conference, SPACE 2024*, pp. 911–915, Jul. 2024, doi: 10.1109/SPACE63117.2024.10668102.

[21] R. Sathe and S. Shinde, "A Deep Learning Framework for Effective Anomaly Detection in Time Series Data," *2024 4th Asian Conference on Innovation in Technology, ASIANCON 2024*, pp. 1–7, Aug. 2024, doi: 10.1109/ASIANCON62057.2024.10837697.

[22] S. Githinji and C. W. Maina, "Anomaly Detection on Time Series Sensor Data Using Deep LSTM-Autoencoder," *IEEE AFRICON Conference*, pp. 1–6, Sep. 2023, doi: 10.1109/AFRICON55910.2023.10293676.

[23] W. Skaf and T. Horváth, "Denoising Architecture for Unsupervised Anomaly Detection in Time-Series," *Communications in Computer and Information Science*, vol. 1652 CCIS, pp. 178–187, 2022, doi: 10.1007/978-3-031-15743-1_17.

[24] J. Hu *et al.*, "Restoration of 1–24 hour dry-bulb temperature gaps for use in building performance monitoring and analysis—Part I," *HVAC&R Res*, vol. 20, no. 6, pp. 594–605, Aug. 2014, doi: 10.1080/10789669.2014.925347.

[25] A. Flores, H. Tito-Chura, O. Cuentas-Toledo, V. Yana-Mamani, and D. Centty-Villafuerte, "PM2.5 Time Series Imputation with Moving Averages, Smoothing, and Linear Interpolation," *Computers 2024, Vol. 13, Page 312*, vol. 13, no. 12, p. 312, Nov. 2024, doi: 10.3390/COMPUTERS13120312.

[26] D. M. Larson *et al.*, "Reconstructing missing data by comparing interpolation techniques: Applications for long-term water quality data," *Limnol Oceanogr Methods*, vol. 21, no. 7, pp. 435–449, Jul. 2023, doi: 10.1002/LOM3.10556.

[27] J. Jin, M. Li, and L. Jin, "Data Normalization to Accelerate Training for Linear Neural Net to Predict Tropical Cyclone Tracks," *Math Probl Eng*, vol. 2015, no. 1, p. 931629, Jan. 2015, doi: 10.1155/2015/931629.

[28] J. Liu, T. Zhang, G. Han, and Y. Gou, "TD-LSTM: Temporal Dependence-Based LSTM Networks for Marine Temperature Prediction," *Sensors 2018, Vol. 18, Page 3797*, vol. 18, no. 11, p. 3797, Nov. 2018, doi: 10.3390/S18113797.

[29] Z. P. Xu, Z. J. Cheng, and B. Guo, "An LSTM Autoencoder-Based Framework for Satellite Telemetry Anomaly Detection," *2022 4th International Conference on System Reliability and Safety Engineering, SRSE 2022*, pp. 231–234, 2022, doi: 10.1109/SRSE56746.2022.10067443.

[30] B. Sauvalle and A. De La Fortelle, "Autoencoder-based background reconstruction and foreground segmentation with background noise estimation," *Proceedings - 2023 IEEE Winter Conference on Applications of Computer Vision, WACV 2023*, pp. 3243–3254, 2023, doi: 10.1109/WACV56688.2023.00326.

[31] A. Jentzen and A. Riekert, "A proof of convergence for stochastic gradient descent in the training of artificial neural networks with ReLU activation for constant target functions," *Zeitschrift fur Angewandte Mathematik und Physik*, vol. 73, no. 5, pp. 1–30, Oct. 2022, doi: 10.1007/S00033-022-01716-W/METRICS.

[32] S. Mastromichalakis, "SigmoReLU: An Improvement Activation Function by Combining Sigmoid and ReLU," Jun. 2021, doi: 10.20944/PREPRINTS202106.0252.V1.

[33] T. O. Hodson, "Root-mean-square error (RMSE) or mean absolute error (MAE): when to use them or not," *Geosci Model Dev*, vol. 15, no. 14, pp. 5481–5487, Jul. 2022, doi: 10.5194/GMD-15-5481-2022.

[34] S. M. Robeson and C. J. Willmott, "Decomposition of the mean absolute error (MAE) into systematic and unsystematic components," *PLoS One*, vol. 18, no. 2, p. e0279774, Feb. 2023, doi: 10.1371/JOURNAL.PONE.0279774.

[35] C. Fung, S. Srinarasi, K. Lucas, H. B. Phee, and L. Bauer, "Perspectives from a Comprehensive Evaluation of Reconstruction-based Anomaly Detection in Industrial Control Systems," *Lecture Notes in Computer Science (including subseries Lecture Notes in Artificial Intelligence and Lecture Notes in Bioinformatics)* , vol. 13556 LNCS, pp. 493–513, 2022, doi: 10.1007/978-3-031-17143-7_24/FIGURES/6.

[36] G. Travieso, A. Benatti, L. Da, and F. Costa, "An Analytical Approach to the Jaccard Similarity Index," Oct. 2024, Accessed: Oct. 14, 2025. [Online]. Available: https://arxiv.org/pdf/2410.16436

[37] Z. Hussain, S. Alam, R. Hussain, and S. ur Rahman, "New similarity measure of Pythagorean fuzzy sets based on the Jaccard index with its application to clustering," *Ain Shams Engineering Journal*, vol. 15, no. 1, p. 102294, Jan. 2024, doi: 10.1016/J.ASEJ.2023.102294.

[38] Y. Wei *et al.*, "Reconstruction-based LSTM-Autoencoder for Anomaly-based DDoS Attack Detection over Multivariate Time-Series Data," Apr. 2023, Accessed: Aug. 23, 2025. [Online]. Available: https://arxiv.org/pdf/2305.09475

[39] A. N. G. R and A. S, "Anomaly Detection of Streamflow Time Series Using LSTM Autoencoder," *Proceedings of the 6th International Conference on Modeling and Simulation in Civil Engineering*, pp. 112–119, Sep. 2023, doi: 10.21467/PROCEEDINGS.156.16.

[40] F. Lachekhab, M. Benzaoui, S. A. Tadjer, A. Bensmaine, and H. Hamma, "LSTM-Autoencoder Deep Learning Model for Anomaly Detection in Electric Motor," *Energies 2024, Vol. 17, Page 2340*, vol. 17, no. 10, p. 2340, May 2024, doi: 10.3390/EN17102340.

[41] J. U. Ko, K. Na, J. S. Oh, J. Kim, and B. D. Youn, "A new auto-encoder-based dynamic threshold to reduce false alarm rate for anomaly detection of steam turbines," *Expert Syst Appl*, vol. 189, p. 116094, Mar. 2022, doi: 10.1016/J.ESWA.2021.116094.

[42] A. Takiddin, M. Ismail, U. Zafar, and E. Serpedin, "Deep Autoencoder-Based Anomaly Detection of Electricity Theft Cyberattacks in Smart Grids," *IEEE Syst J*, vol. 16, no. 3, pp. 4106–4117, Sep. 2022, doi: 10.1109/JSYST.2021.3136683.

[43] Y. Wei, J. Jang-Jaccard, W. Xu, F. Sabrina, S. Camtepe, and M. Boulic, "LSTM-Autoencoder-Based Anomaly Detection for Indoor Air Quality Time-Series Data," *IEEE Sens J*, vol. 23, no. 4, pp. 3787–3800, Feb. 2023, doi: 10.1109/JSEN.2022.3230361.

[44] T. Wahyono, Y. Heryadi, H. Soeparno, and B. S. Abbas, "Anomaly Detection in Climate Data Using Stacked and Densely Connected Long Short-Term Memory Model," *J Comput (Taipei)*, vol. 31, no. 4, pp. 42–53, 2020, doi: 10.3966/199115992020083104004.

[45] G. Fan, Y. Ma, J. Huang, X. Mei, and J. Ma, "Robust graph autoencoder for hyperspectral anomaly detection," *ICASSP, IEEE International Conference on Acoustics, Speech and Signal Processing - Proceedings*, vol. 2021-June, pp. 1830–1834, 2021, doi: 10.1109/ICASSP39728.2021.9414767.

[46] R. Kuzu *et al.*, "An Unsupervised Anomaly Detection Problem in Urban InSAR-PSP Long Time-series," *EGU23*, Feb. 2023, doi: 10.5194/EGUSPHERE-EGU23-13106.

[47] M. Li, Y. Li, K. Cao, and B. Han, "Anomaly Detection of Ecological Monitoring Data Based on Long and Short-Term Memory Network-Autoencoder," *2024 5th International Seminar on Artificial Intelligence, Networking and Information Technology, AINIT 2024*, pp. 962–965, 2024, doi: 10.1109/AINIT61980.2024.10581663.

[48] L. Wong, D. Liu, L. Berti-Equille, S. Alnegheimish, and K. Veeramachaneni, "AER: Auto-Encoder with Regression for Time Series Anomaly Detection," *Proceedings - 2022 IEEE International Conference on Big Data, Big Data 2022*, pp. 1152–1161, 2022, doi: 10.1109/BIGDATA55660.2022.10020857.

[49] H. A. Alif, P. Kamaraj, M. Assaduzzaman, and A. D. Nath, "Spatio-Temporal Deep Neural Modelling for Climate Anomaly Detection using CNN-LSTM Networks," pp. 1196–1202, Sep. 2025, doi: 10.1109/ICSCSA66339.2025.11171200.

[50] Z. K. Shahid, S. Saguna, and C. Åhlund, "Autoencoders for Anomaly Detection in Electricity and District Heating Consumption: A Case Study in School Buildings in Sweden," *Proceedings - 2023 IEEE International Conference on Environment and Electrical Engineering and 2023 IEEE Industrial and Commercial Power Systems Europe, EEEIC / I and CPS Europe 2023*, 2023, doi: 10.1109/EEEIC/ICPSEUROPE57605.2023.10194605.

[51] H. Akbarian, I. Mahgoub, and A. Williams, "Autoencoder-LSTM Algorithm for Anomaly Detection," *2023 IEEE 20th International Conference on Smart Communities: Improving Quality of Life using AI, Robotics and IoT, HONET 2023*, pp. 216–221, 2023, doi: 10.1109/HONET59747.2023.10374710.

[52] S. Githinji and C. W. Maina, "Anomaly Detection on Time Series Sensor Data Using Deep LSTM-Autoencoder," *IEEE AFRICON Conference*, 2023, doi: 10.1109/AFRICON55910.2023.10293676.

[53] M. Li, Y. Li, K. Cao, and B. Han, "Anomaly Detection of Ecological Monitoring Data Based on Long and Short-Term Memory Network-Autoencoder," *2024 5th International Seminar on Artificial Intelligence, Networking and Information Technology, AINIT 2024*, pp. 962–965, 2024, doi: 10.1109/AINIT61980.2024.10581663.

[54] A. Ramírez-Rojas *et al.*, "Anomaly Detection in Fractal Time Series with LSTM Autoencoders," *Mathematics 2024, Vol. 12, Page 3079*, vol. 12, no. 19, p. 3079, Oct. 2024, doi: 10.3390/MATH12193079.

[55] S. Erniyazov, Y. M. Kim, M. A. Jaleel, and C. G. Lim, "Comprehensive Analysis and Improved Techniques for Anomaly Detection in Time Series Data with Autoencoder Models," *Int J Adv Sci Eng Inf Technol*, vol. 14, no. 6, pp. 1861–1867, Dec. 2024, doi: 10.18517/IJASEIT.14.6.20451.

[56] P. Wiessner, G. Bezirganyan, S. Sellami, R. Chbeir, and H. J. Bungartz, "Uncertainty-Aware Time Series Anomaly Detection," *Future Internet 2024, Vol. 16, Page 403*, vol. 16, no. 11, p. 403, Oct. 2024, doi: 10.3390/FI16110403.

[57] B. Yuniasih, W. Nusa Harahap, D. Agung Satya Wardana Prodi Agroteknologi, F. Pertanian, and I. Pertanian Stiper Yogyakarta, "Anomali Iklim El Nino dan La Nina di Indonesia pada 2013-2022," *AGROISTA : Jurnal Agroteknologi*, vol. 6, no. 2, pp. 136–143, Feb. 2022, doi: 10.55180/AGI.V6I2.332.